aerospace

MDPI

Article

The Impact of Dispatch Weight Restrictions on Derivative Aircraft Propulsion Technology Evaluation

Timothy T. Takahashi

Department of Aeronautics & Astronautics, Air Force Institute of Technology, Wright-Patterson AFB, OH 45433, USA; timothy.takahashi@afit.edu

Abstract

This paper arises from an ARPA-E-sponsored project seeking design opportunities to retrofit existing aircraft with hybrid electric propulsion systems. Engineers typically configure aircraft to fly a given payload over a long range, which is subject to field performance constraints. In practice, operators fly transport aircraft (civilian and military) in a manner where dispatch consciously trades payload and/or range to enable safe operations to and from short runways. This work describes a simple yet novel analytical process suitable for inclusion in conceptual design or technology portfolio trade study evaluations to assess the impacts of weight-restricted dispatch upon usable payloads. We find that options that increase low-speed thrust may maintain or improve the useful payload even if it substantially increases aircraft fixed weight. Conversely, otherwise desirable technologies that decrease low-speed thrust may severely impact the useful payload of aircraft operating to and from short runways.

Keywords: take-off; dispatch; flight mechanics; civil aviation; military aviation

1. Introduction

For many years, industry has used analytical data to inform strategic technology portfolio investment [1]. Such decision-making information traditionally arises from the application of focused empirical adjustments to components within "conceptual design"-level aircraft performance and sizing tools [2]. In itself, "technology" is an abstract concept that influences aircraft configuration through its impact on subsystems size, weight, power (SWAP), and/or efficiencies. Ideally, the customer imposes high-level requirements which drive the final design; form follows function [3–10]. Alternatively, the customer may accept or decline the offered product. In either scenario, the integration of complex subsystems is an important issue in aircraft design. Subsystem SWAP and other attributes may impose or relax constraints on other subsystems as well as on the overall aircraft system performance.

This paper arises from ARPA-E-sponsored project work to evaluate derivative aircraft design opportunities to utilize high-powered (>2 MW) flight weight electric motors [11]. AFIT has been commissioned to study the utility of a hybrid electric retrofit to the Lockheed C-130 [12]. In the process of executing this contract, we at AFIT realized that many existing hybridization technology portfolio studies [13–15] did not consider the reality that tactical transport aircraft often operate far below their certified maximum take-off weight in order to satisfy strict field performance constraints.

This observation motivates a more generalized research question: How does the intentional operation of an aircraft where the end user trades payload and/or range for field performance impact broader sizing or technology portfolio trade studies? In this work,

Check for updates

Academic Editors: Carlo E. D. Riboldi and Konstantinos Kontis

Received: 5 March 2026
Revised: 27 April 2026
Accepted: 18 May 2026
Published: 20 May 2026

Copyright: © 2026 by the author. Licensee MDPI, Basel, Switzerland. This article is an open access article distributed under the terms and conditions of the Creative Commons Attribution (CC BY) license.

we show how operational constraints affect how technologies should be judged. A related student thesis evaluated mission effectiveness, environmental and operating-cost impacts of select hybrid electric propulsion technologies applied to a C-130 [12].

This work exercises a broad semi-empirical field performance model developed by the author [16] to support the following thesis: under a weight-restricted dispatch, three engineering variables dominate the design. The critical parameters are: (1) the low-speed, take-off-power thrust from the propulsion system; (2) the fixed-weight impact of the proposed technology; and (3) the potential fuel savings arising from the proposed technology, as evaluated over the short-range mission. Based on the nature of the restriction (originating airport field length, originating airport obstacle clearance, arrival airport field length), this new method provides insight into the useful payload as a function of thrust, weight and fuel savings. This conceptual perspective should help inform future studies.

2. Technology Portfolio Trades

In an ideal setting, clean-sheet aircraft design is a process where engineers transform requirements into physical hardware. Model-Based Systems Engineering (MBSE) advocates a design process informed and substantiated by coupled numerical models [17]. By its very nature, aircraft design is highly multi-disciplinary; a successful design must balance aerodynamics (of external as well as internal flows), acoustics, thermodynamics, materials science, electrical engineering, machine and mechanism design, and manufacturing engineering. As such, these studies grew out of a field of study once called Operations Research.

2.1. Connection Between Operations Research and Aircraft Technology Roadmapping

Operations Research made its name during the Second World War when former U.S. Defense Secretary, Robert McNamara, and his "whiz kids" were tasked to develop scientific methods to provide "executive departments with a quantitative basis for decisions regarding the operations under their control" [18,19]. A famous early study selected the size of transport ship convoys to minimize vulnerability to German U-boats. Operations Research provided counterintuitive insight, showing that vulnerability was most correlated with the number of escort vessels present, rather than the size of the convoy [20].

By the late 1950s, Operations Research principles began to broadly influence how engineers tackled the generalized design process. Professor Lucien Schmit led the transformation of engineering design from an analytical (calculus- and asymptotic-expansion-based methods) pursuit to one involving direct numerical solutions of relevant performance parameters [21].

Beginning around the millennium, Mavris & Kirby at Georgia Tech applied aircraft multi-disciplinary optimization (MDO) methods to inform the financial allocation of aviation research and development efforts [1,22,23]. Their innovation was to provide a numerical basis to guide the decision-making process for program initiatives and capital project investments [1]. Their formulation relied on modeling aerospace "technology" through empirical changes (either benefitting or degrading) component weights, drag, fuel flow, thrust, cycle parameters, engine efficiencies, subsystem weights, and economic parameters (i.e., fuel or labor costs) [1].

Mavris & Kirby introduced the concept of using empirical *k-factors* to model incremental changes in technical disciplinary metrics, which feed coupled MDO models [1]. A *k-factor* of zero represents an established nominal value for scalar (i.e., empty weight) or vector (*CL* vs. *CD* drag polar) engineering data; a negative value is associated with optimism (i.e., a *k-factor* of −25% on *CD0* would revise all drag polars to reflect a 25% reduction in zero-lift drag). When used in a technology portfolio study, human consensus would establish a collection of specific *k-factors* to represent a particular concept. For example, a

propulsive system technology like exhaust nozzle chevrons would be assigned to a collection of impact factors for empty weight, non-recurring cost, flyover noise, thrust and *TSFC*. Their associated MDO model propagates these effects across other disciplines; its output can be assessed quantitatively through a "prediction profile" scatter plot; see Figure 1.

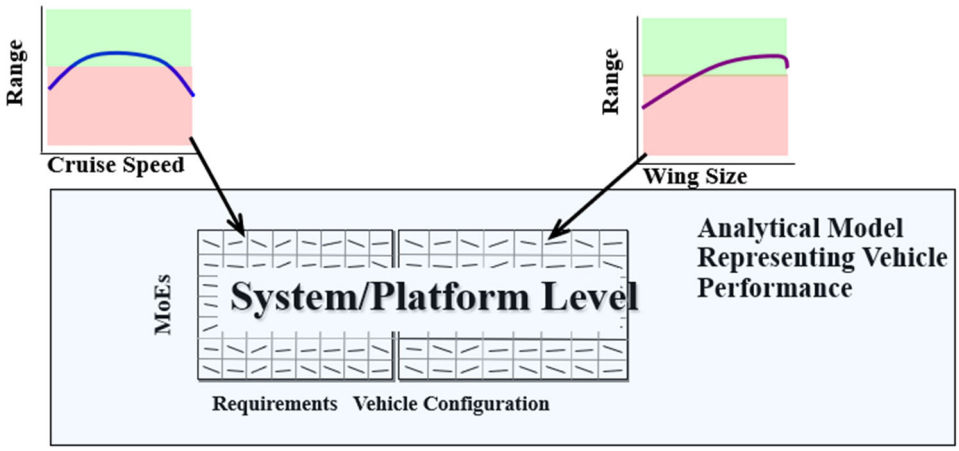


Figure 1. System-level sensitivities to design variables for a notional aircraft.

Powered by an underlying aircraft MDO model, off-the-shelf statistical analysis software like JMP can enable decision-makers to learn how different technology areas interact with system performance metrics [24]. If a leader decides that a technology *k-factor* broadly improves predicted system performance, that particular technology can be given further financial support. Indeed, Cavanaugh highlights this process as one that a combined NASA/NIA/Georgia Tech team embraced [25].

Over the following 25 years, we note that the vast majority of openly published technology portfolio studies stem from Professor Mavris' laboratory. The underlying MDO model has included, at various times, FLOPS [26,27], Pacelab Suite [2], in-house hybrid/electric performance codes [28]. Other university groups, such as TU Braunschweig, have retraced the Georgia Tech basic technology portfolio trades (drag reduction, propulsion efficiency, and structural weight reduction concepts) using their own modeling codes [29]. Similarly, Lim et al. at Seoul National University applied Kirby & Mavris' basic framework to examine small electric air mobility vehicle technologies [30].

In industry, SAAB in Sweden has openly embraced the technology portfolio approach. Over the past decade, Amadori and his collaborators have regularly published an evolving understanding of how to better visualize MDO-derived data (beyond JMP) to reveal how technology impacts complex system performance [31–34]. At the present, none of their exemplary studies have considered an obviously field-performance-constrained design challenge.

2.2. Recent Interest in the Application of Hybrid Electric Propulsion Technology to Retrofit Existing Aircraft

A number of teams have recently published both point-design and technology portfolio trade study results considering retrofit electric propulsion to existing transport aircraft. We refer to the reader a recent and very comprehensive review article by Abu Salem et al., which covers a broad gamut of clean-sheet and derivative aircraft proposals [35]. In this section, we highlight a few representative studies.

Friedrich & Robertson considered a hybrid electric propulsion retrofit of a Boeing 737–800 airframe [36]. They explored options with a pair of resized core turbofans using either 1 or 2 MW electric motors to assist the turbofans. They also presume the availability of 750 (W·h)/kg energy density batteries. Their options required an increase in MTOW

to offset a substantial increase in fixed weight arising from the hybridization and the need for large batteries. While they did not detail field performance constraints, they did upsize the total thrust of their engines approximately 13% in order to maintain a desired all-engines-operating climb profile.

Wroblewski & Ansell considered a hybrid drivetrain retrofit to a Boeing 737–700 airframe [37]. To close their design, they suggested a 50% electrical-power drivetrain—where electric power is added to the low-pressure spool of a downsized gas turbine core—along with 1000 (W·h)/kg energy density batteries as being appropriate to perform a wide range of missions. They mention field performance only in passing; they did not explicitly consider the impact of their proposed retrofit on take-off or landing performance.

Voskuhi et al. considered a hybrid electric regional turboprop aircraft configuration strongly reminiscent of an ATR-72-600 [38]. They analyzed a point-design with a 34% electrical power ratio drivetrain and 1000 (W·h)/kg energy density batteries. Their proposed solution had both a 14% increase in *MTOW* and an 18% increase in *Sref* compared to the baseline, primarily due to the battery mass needed to fly the ~1300 NM reference mission. They did not explicitly consider take-off or landing performance in their study.

Antcliff et al. considered a hybrid electric regional turboprop aircraft configuration derived from an ATR-42-500 [39]. In order to keep their study manageable, they held the ATR-inspired fuselage geometry and engine size (2400-ESHP per engine) fixed and varied the *MTOW*, wing size, tail size (holding tail volumes constant), and propulsion hybridization fraction. With 500 (W·h)/kg energy density batteries, their study found that an aircraft sized for a 7000 ft runway required a substantial increase in the wing area (more than double) and gross weight (more than double) to perform a 600 NM economic mission. Battery weight for storing the necessary energy was their major design driver.

Recine et al. utilized a modified version of the NASA/Ames sizing code GASP to analyze the Boeing 737-MAX8 and the Embraer E190-E2 as possible foundations for future electric propulsion flight demonstrators [40]. Their formulation follows Kirby & Mavris with the application of *k-factors* to aerodynamics, structures, and propulsive system performance to assess suitability. However, they did not include scenarios where either aircraft was operated in a weight-restricted manner.

Pham et al. used GASP to study a different application, a Lockheed C-130H where two turboprop engines would be exchanged for two battery/electric propulsors [13]. Although their reference mission did not impose a field performance restriction on weight, their team's work specifically demonstrated how motor and battery scaling could improve or degrade field performance [13].

Listgarten et al. published a related study, reverse-engineering a DeHavilland DHC-8 Q400 [14]. Their group indicated significant possible fuel savings from hybridization (i.e., electric assist) but did not otherwise discuss its impact on field performance [14]. Most recently, Jansen published a follow-up study for a proposed C-130H modification [15]. This was a point-design study with greater subsystem detail of a "true parallel" concept—with two fossil fuel turboprops and two battery/electric propulsors [15]. Unlike Pham's earlier study, this paper did not discuss impacts on field performance.

As noted in the introduction, ARPA-E's interest in the near-term application of state-of-the-art battery/electric technology retrofits of existing aircraft motivates this paper [11]. Among the commercial airliners speculated for possible conversion, all three types (737, Q-400 and E190) regularly fly weight-restricted economic missions. Among the dual-use aircraft contemplating conversion, the Lockheed L-100/C-130 is likely to be flown in a weight-restricted manner in peacetime as well as in tactical operations.

3. Aircraft Sizing Considering Weight-Limited Dispatch

Engineers configure aircraft to transport a defined payload over a still-air mission range from an originating airport to a destination airport. Field performance inserts itself into the design process, since operational regulations prohibit dispatch of an aircraft with insufficient performance to achieve safe flight in the event of an engine failure.

Aircraft mission capabilities are typically summarized through a payload–range chart; see Figure 2 [6]. Conventional aircraft sizing [4–10] emphasizes capabilities to achieve the desired payload at range for dispatch at maximum take-off weight (MTOW); see the blue dot in Figure 2. In practice, it is common for aircraft to fly a reduced payload over a shorter range from a short runway (the red dot on Figure 2). The maximum payload capability is defined by certification structural limits, which specify the maximum zero-fuel weight (*MZFW*) and the maximum landing weight (*MLW*). Flights where dispatch (rather than design) consciously restricts the capability to achieve necessary field performance are known as "weight-restricted" operations.

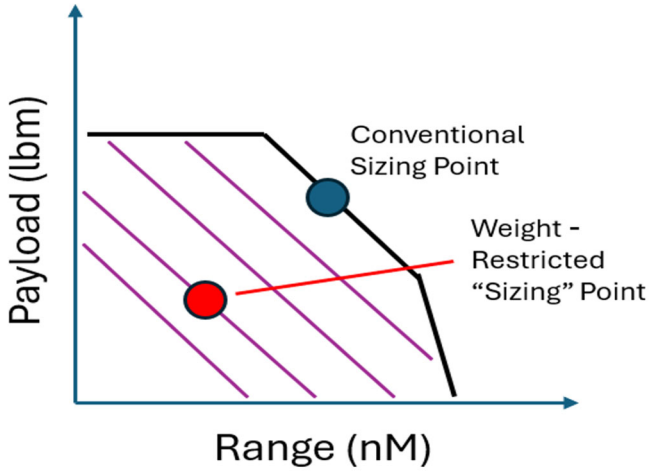


Figure 2. Classical payload–range chart. Engineers design aircraft to transport a payload over a given range for departure at maximum take-off weight (*MTOW*) (the blue dot). Aircraft dispatch may weight-restrict both payload and range to improve field performance (the red dot).

Operationally, weight-restricted dispatch is more common than textbooks otherwise suggest. Dispatch may limit payload to achieve field performance capabilities for safe take-off, obstacle clearance, or landing. Such conditions often arise due to weather: (1) high ambient temperatures or gusty winds that necessitate take-off at reduced flap settings, (2) hot weather or bleed diversion due to icing conditions that reduce available thrust, and (3) gusty winds that necessitate landing at reduced flap settings. Alternatively, strong headwinds aloft can increase the required fuel load. Because complex terrain surrounds many airports, dispatch may require engine-inoperative climb gradient capability in considerable excess of the minimum regulatory requirements (2.4% for twin-engine 14 CFR § 25 aircraft and 2.5% for multi-engine MIL-3013 aircraft) [41,42].

Some airports regularly lead to weight-restricted dispatch while others will limit only during exceptional weather events. London City Airport (EGLC) is a famous example; although it is located near sea level and has few obstacles, its runway (4948 ft) is considerably shorter than the advertised standard-day *MTOW* field length of the Embraer 190 (~7400 ft) which operator British Airways heavily utilize [43,44]. Toronto Billy Bishop (CYTZ) is another example, with its 4000 ft long runway (8/26); this is considerably shorter than the ~4700 ft advertised standard-day *MTOW* field length of the Bombardier DHC-8 Q400, which the dominant operator, Porter Airlines, regularly utilizes [45,46].

Airlines have acquired substantial aircraft fleets, which must be weight-restricted to fly regularly scheduled routes. For example, Southwest Airlines is a major operator of the Boeing 737-MAX8 (more than 273 in service), with an advertised ~8300 ft sea-level standard-day *MTOW* field length; Southwest routinely uses this aircraft to fly to and from airports such as John Wayne (KSNA) with a 5700 ft runway, Santa Barbara (KSBA) with a 6052 ft runway and Chicago/Midway (KMDW), with its longest runway (13L/31R) at 6522 ft [47–50]. All flights to and from these major airports must be weight-restricted to depart considerably lighter than *MTOW* and possibly arrive considerably lighter than *MLW*.

Weight-limited dispatch poses an interesting constraint to the concept of a "technology portfolio trade" because all attributes of the study must be seen through the prism of field performance. In general, technology portfolio trades try to identify unforeseen synergies across many different metrics. In the world of field performance, very few things matter: basically, weight, thrust and thrust-lapse, wing area, *CLmax*, and sometimes minimum control speed. Absent a benefit to thrust or stall speed, every additional pound of fixed weight must be offset with a reduction in fuel burn or payload.

Figure 3 is a schematic of how dispatch determines a need for a weight-limited departure. The originating airport has a defined runway (based on ground winds) which implies a maximum take-off distance (which is a function of outside air temperature and pressure altitude). This runway will also define a minimum engine-inoperative take-off climb gradient to ensure safe obstacle clearance. The destination airport has a known available runway length based on climatic conditions. The origination and destination airports are separated by a "still-air-distance" based on planned air-traffic routing and winds aloft; this implies a take-off-weight-dependent fuel burn. The maximum permissible dispatch weight is limited by one of the following constraints: (1) it cannot exceed the maximum certified take-off weight of the aircraft (*MTOW*); (2) it cannot exceed the maximum weight implied by the available take-off-distance (*TODA*) given the weather at the time of departure; (3) it cannot exceed the maximum weight implied by the engine-inoperative climb gradient given the weather at the time of arrival; (4) after it consumes mission fuel, it cannot exceed the maximum certified landing weight of the aircraft (*MLW*); and (5) after it consumes mission fuel, it cannot exceed the maximum weight implied by the available landing distance (*LDA*) given the anticipated weather at the time of arrival.

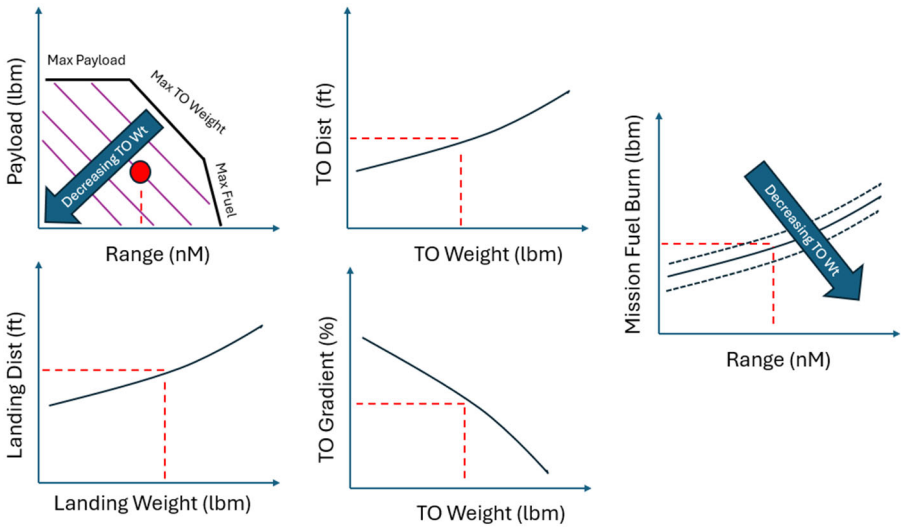


Figure 3. Constraints which drive weight-limited dispatch.

4. Analytical Modeling Basis

As noted in the Introduction, weight-limited dispatch may impact the operational and/or economic utility of an aircraft. Because weight limitation due to a field performance requirement is a multi-faceted constraint, its impact is context-dependent. For example, some operations have desired payload and fuel loads that fall below any weight limits for dispatch; they are unconstrained. If constraints are active, they overwhelm any other contributor to an objective function (for example, a desire to minimize fuel burn per unit payload). Under weight-limited dispatch constraints, the operator might be required to limit take-off to only a fraction of the intended payload.

4.1. Runway and Obstacle Clearance Nomenclature

To illustrate real-world constraints, let us consider two runways in Southern California: (1) Santa Barbara (KSBA), a commercial airport with regularly scheduled B737-MAX8 operations; and (2) Agua Dulce (K70), near the Vasquez Rocks, a rural general-aviation airport, which is a possible destination for peace-time military (natural disaster/med-evacuation) C-130 flights.

For the B737-MAX8, FAA operations from Runway 7 imply take-off (*TODA*) and landing (*LDA*) within 6052 ft at sea level. FAA IFR departure guidelines require a minimum climb capability of 260 ft/NM (i.e., 4.3%) through 1100 ft AGL [49].

For the C-130, a departure from Runway 4 at Agua Dulce requires safe take-off and landing (*TODA* and *LDA*) from a 4205 ft runway at 2633 ft MSL. Agua Dulce is surrounded by significant terrain (up to 5200 ft MSL); see Figure 4. This implies a minimum of ~600 ft/NM (i.e., ~10%) climb gradient to safely overfly [51].

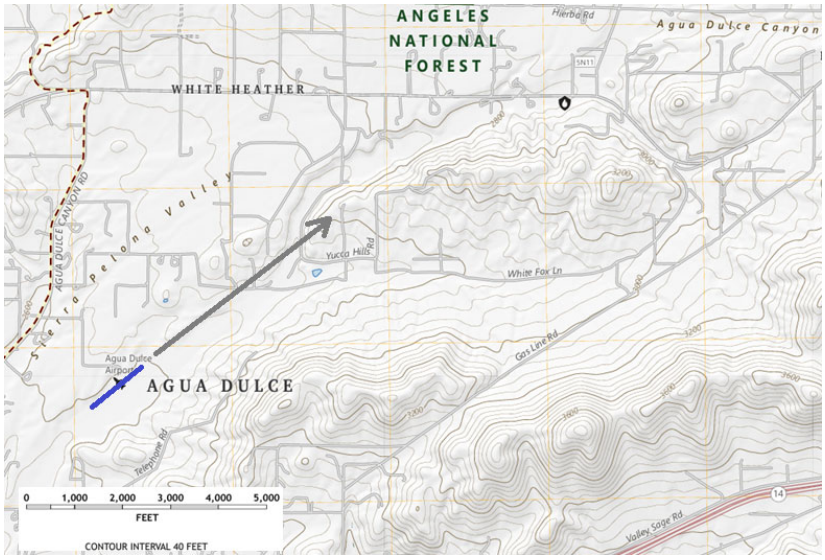


Figure 4. Excerpt from a topographic map showing the terrain surrounding Agua Dulce (L70) [52]. Image adapted from a public domain map provided by the U.S. Geological Survey.

4.2. Propulsive System Modeling

Propulsive system technology portfolio trades for derivative aircraft operated in a weight-restricted manner must consider size, weight, and power impacts on the airframe. The sizing limits (i.e., propeller overlap, nacelle ground strike) may impose physical scaling constraints for any given technology. The weight involves both the mechanical fitment of the propulsor plus any supplemental energy storage system (alternative fuel, fuel cells, batteries) and related subsystems (cryogenics and other thermal management systems, wiring, etc.). The power involves both static and dynamic thrust (lapse rates with speed

and altitude) of the propulsor itself, as well as the energy-consumption characteristics of the technology (whether the technology is used to assist take-off, climb, cruise or is required for the entire mission).

In general, changes in propulsive system technology should not radically impact the maximum lift coefficient (*CLmax*) of an airframe. While this study does not consider possible impacts on *CLmax* or synergies associated with propulsion trade studies, future work should consider potential cross-disciplinary effects. The C130-J has a lower *CLmax* than a C-130H because it requires a stick-pusher to mitigate degraded bare-airframe stall characteristics associated with its engine/propeller change [53]. Similarly, the nacelle changes between the B737-NG and the B737-MAX altered flying qualities enough to motivate Boeing to develop the MCAS system [54].

To highlight general trends, this study will define the impact of a propulsion system technology change in terms of three "*k-factors*:" (1) the % change in low-speed, take-off power thrust, (2) the % change in *OEW* (including battery weight), and (3) the % change in mission *TSFC*. For example, a noise-suppressing inlet treatment might decrease take-off thrust by 2%, increase *OEW* by 0.2% *MTOW* (i.e., 100 lbm) and increase mission fuel consumption by 0.1%. Alternatively, a candidate hybrid electric propulsion system retrofit might increase take-off thrust by 10%, increase *OEW* by 30% *MTOW* (i.e., 30,000 lbm) and decrease mission fuel consumption by 25%.

4.3. Weight Nomenclature That Decouples Operational Take-Off and Landing Weights from Structural Certification Weights

While structural certification compliance specifies a maximum take-off weight (*MTOW*) and maximum landing weight (*MLW*), real-world operations rarely schedule aircraft to approach these limits. In regular usage, aircraft depart at a given take-off weight and land at a given landing weight. The operational take-off and landing weights as used by dispatch may be derived from the following relationships:

$$TOW = OEW + PAYLOAD + MISSIONFUEL + RESERVEFUEL \quad (1)$$

and

$$LW = OEW + PAYLOAD + RESERVEFUEL \quad (2)$$

where *OEW* is the aircraft operational empty weight and *RESERVEFUEL* is the weight of the fuel needed to fly from the destination airport to the declared alternate safe-harbor and hold for at least the regulatory specified minimum time period (45 to 60 min, depending on the operational standard). The payload cannot exceed the maximum value implied by the difference between the maximum zero-fuel weight and the operational-empty-weight (*MZFW-OEW*). Similarly, dispatch will disallow operations where the planned landing weight (*LW*) exceeds the certified maximum landing weight (*MLW*). Field performance limitations may arise from several sources: (1) take-off from a short *TODA* may limit the take-off-weight; (2) take-off requiring a steep climb gradient may limit the take-off-weight; and (3) limitations arising from a short-arrival *LDA* may restrict the landing weight.

4.4. Simplified Model to Estimate Mission Fuel Associated with the Desired Mission

For the purposes of this paper, we use a highly simplified analytical model to estimate fuel savings. In more detailed follow-up trade studies, we can estimate fuel consumption using a time-step integrating simulation that models a complete reference mission, including take-off, climb, cruise, descent, approach, and landing [10].

For range, we begin with the Breguet equation:

$$RANGE = \frac{VKTAS}{TSFC}\left(\frac{L}{D}\right)\log_e\left(\frac{OEW + PAYLOAD + MISSIONFUEL + RESERVEFUEL}{OEW + PAYLOAD + RESERVEFUEL}\right) \quad (3)$$

Next, algebraically reshuffle the terms to solve for mission fuel in terms of the other parameters:

$$MISSIONFUEL = (OEW + PAYLOAD + RESERVEFUEL)\left[exp\left(\frac{RANGE\ TSFC}{VKTAS\left(\frac{L}{D}\right)}\right) - 1\right] \quad (4)$$

We can then introduce the *k-factors* into this formulation as:

$$MISSIONFUEL = (OEW\ + MTOW\,k_{OEW} + PAYLOAD + RESERVEFUEL)\left[exp\left(\frac{RANGE\ TSFC\ (1 + k_{TSFC})}{VKTAS\left(\frac{L}{D}\right)}\right) - 1\right] \quad (5)$$

The sign convention in our nomenclature has $k_{TSFC} = -0.5$ representing the halving of fuel flow and the doubling of efficiency. Similarly, $k_{OEW} = +0.10$ represents an increase in *OEW* commensurate with 10% of *MTOW*. *RANGE* is critical to the end-user; the longer the mission, the greater the amount of required mission fuel. For a derivative aircraft, flight speed and aerodynamic efficiency are unlikely to change appreciably from the baseline.

Mission specific range (NM/lbm fuel consumed) can be inferred:

$$SPECIFICRANGE = \frac{RANGE}{MISSIONFUEL} \quad (6)$$

4.5. Empirical Model to Estimate Take-Off Field Performance

We estimate take-off distance using the author Takahashi's recently published improved method to predict the Critical Field Length, *CFL* [16]. For safe operations, the available runway must always exceed the critical field length, *TODA* > *CFL*. These simplified equations have been validated against a broad collection of numerical simulations and certified flight manual data, including the sorts of *T/W* contemplated here. For both military and civilian aircraft, take-off field performance has been found to be a function of:

$$TOP = \frac{\left(\frac{W}{Sref}\right)}{\left(\frac{T}{W}\right)CL_{max}} \quad (7)$$

where *TOP* is the square of the take-off weight (*W*) divided by the wing area (*Sref*), static thrust of the propulsion with all engines operating (*T*) and the maximum lift coefficient (*CLmax*). We introduce our quantity of thrust *k-factor* as:

$$T = T_{AEO_{STATIC}}(\,1 + k_{THRUST}). \quad (8)$$

For FAA operations on dry runways:

$$CFL_{14CFR25_DRY} = \max(\,750 + 31\ TOP,\ 3300). \quad (9)$$

For MIL-STD-3013B operations on dry runways:

$$CFL_{3013B_DRY} = \max(250 + 38\ TOP,\ CFLmin_{3013B_DRY}), \quad (10)$$

where the minimum-control-speed (*VMCA*) floor on decision speed limits *CFL* to a distance no less than:

$$CFLmin_{3013B_DRY} \approx 5525 - 58VMCA + 0.44VMCA^2 \quad (11)$$

Through the estimation of *CFLmin*, this model accurately captures the stability and control impacts arising from increased *OEI* thrust. For the scenarios discussed in this paper, our field length requirements are strenuous enough to limit dispatch weight but not so strenuous as to run into probable *VMCA* limitations.

One design decision intentionally left vague involves the basic topology of any proposed hybrid electric retrofit: whether to engineer a true-parallel hybrid (where an electric propulsor replaces a liquid-fuel engine) or a series hybrid (where a redesigned power module would include both liquid fuel and electric elements). All aircraft are amenable for series hybrid conversions. Alternatively, true-parallel hybrid architectures are the easiest to implement on a four-engine aircraft like a C-130, where one could retain a pair of liquid-fuel engines and swap over two fully electric propulsion modules.

The definition of engine-inoperative performance under a true-parallel hybrid architecture is clear-cut: either a liquid-fuel or an electric power module can fail. The complete thrust loss of that propulsor must be accounted for when computing field performance (runway and obstacle clearance). The definition of engine-inoperative performance under a series hybrid architecture is less obvious with each propulsion module containing both liquid-fuel and electric elements.

For the reference C-130 short-field mission, Eqn. 11 indicates that it is important to retain *VMCA* < ~102 knots for safe dispatch from a 4205 ft runway, although scheduled obstacle clearance speeds at typical flight weights vary from ~120 to ~140 knots. The production C-130J already incorporates a complex automatic take-off thrust control system (*ATTCS*) with an airspeed-scheduled thrust derate, which engages only upon sensed engine failure [55]. When *ATTCS* senses the failure of an outboard engine, it may reduce the thrust on an opposing healthy engine to limit unsymmetric moments. As aerodynamic control power increases with the square of the airspeed, the system will restore power. Maximum derate occurs at *VMCA*. At 120 knots, aerodynamic control power is 60% greater than at the official *VMCA,* which is 95 knots. At 130 knots, aerodynamic control power is 87% greater than that at 95 knots. Since our trade studies consider up to a 60% increase in take-off thrust over baseline, it seems reasonable that *ATTCS* scheduling can restore full thrust on all operating engines once airborne, while keeping *VMCA* < 102 knots. For moderate increases in *T/W*, a series hybrid replacement of the inner C-130 engines to include electrical assistance seems practical. For more extreme increases in *T/W*, the replacement of all four C-130 engines to include electric assistance makes more sense. It is critical that detail design does not ignore *VMCA* considerations.

4.6. Empirical Model to Estimate Landing Field Performance

Landing performance distances will be estimated using author Takahashi's further revisions to Roskam's empirical equations [56,57]. For safe operations, the available landing distance (*LDA*) must always exceed the predicted distance for landing.

For FAA operations on a dry runway under the "167% actual landing distance" rule, we may correlate the landing reference speed with the available runway as:

$$LDA > 1586 + 0.184\ V_{REF}^2 \tag{12}$$

where V_{REF} = max (1.23 V_S, *VMCL*) in the landing configuration.

When following MIL-3013B rules on a dry runway, we correlate the final, powered approach speed with the available runway as:

$$LDA > \max(825 + 0.150{V_{PA}}^2,\ 1000) \tag{13}$$

where V_{PA} = max (1.2 V_S, 1.05 *VMCL)* in the landing configuration.

We may estimate sea-level standard-day stall speed in knots:

$$V_S = 660.8 \sqrt{\frac{\frac{W}{Sref}}{1481\ CLmax}} \tag{14}$$

4.7. Estimation of Engine-Inoperative Climb Gradient

We may estimate the engine-inoperative climb gradient using the classic small-angle approximation work-energy theorem:

$$GRAD \approx 100\% \frac{T_{OEI} - D}{W} \tag{15}$$

where T_{OEI} is the dynamic thrust of the remaining engines flown at the scheduled second-segment climb speed; *D* is the drag at the second-segment climb speed ($D = (CD0 + CL^2/(\pi\ ARe)$)

$((V_2/660.8)^2/1481)$ *Sref*); and *W* is the dispatch weight. The speeds differ between certification bases: V_2 = max (1.13 *Vs*, 1.1 *VMCA*) for 14 CFR § 25 aircraft and V_{OBS} = max (1.2 *Vs*, 1.05 *VMCA*) for MIL 3013-B aircraft.

For this study, we share our quantity of the thrust *k-factor* with the take-off equation:

$$T_{OEI} = T_{OEI_{DYNAMIC}}(1 + k_{THRUST}). \quad (16)$$

Based on previous experience with vendor-supplied engine decks, we may define a relationship between $T_{AEO_{STATIC}}$ and $T_{OEI_{DYNAMIC}}$. This study will presume that the dynamic thrust of an ultra-high-bypass ratio turbofan is ~80% of its static thrust at typical initial take-off climb speeds, whereas a turboprop will lapse to ~70% of its static thrust. *OEI* thrust will be based on ½ the *AEO* thrust for the B737 and ¾ the *AEO* thrust for the C-130 (based on the premise that ATTCS thrust reductions are not active at realistic climb-out airspeeds). Thus, the *OEI* climb-out thrust for the B737-inspired configuration is 40% of the *AEO* static thrust; for the C-130-inspired configuration, the *OEI* dynamic thrust is 52.5% of the *AEO* static thrust.

5. Simplified Propulsive System Technology Portfolio Trades

In this section, we examine propulsive system technology trades as applied to several aircraft and operational scenarios: (1) a 737-MAX8-inspired commercial airliner flown over a ~1500 NM stage from KLAX to KMDW, (2) a weight-restricted 737-MAX8-inspired commercial airliner flown over a ~500 NM stage from KSBA (6052 ft runway) with a 4.3% *OEI* climb gradient, (3) a C-130-inspired aircraft flown over a ~1500 NM stage from KLAX, and (4) a C-130-inspired aircraft flown over a ~500 NM stage from a 4000 ft runway with a 10% *OEI* climb gradient to another 4000 ft runway. We will see how interacting constraints may or may not impact the operational and economic utility of these aircraft.

An examination of the terms in Equations 1 through 16 reveals that, for all weight-restricted dispatch studies, the only *k-factors* that are active are those which impact the aircraft empty weight (k_{OEW}), alter the quality of thrust (k_{TSFC}), and/or alter the quantity of thrust (k_{THRUST}). Thus, all generalized technology portfolio trades need to include these three terms at minimum, among the many other potential *k-factors* (for cost, noise, environment, maintenance, etc.).

For the study of immediate interest to AFIT, the hybrid electric retrofit of transport aircraft, we first sought to identify the nature of favorable and unfavorable interactions between the critical *k-factors.* Due to energy density limitations of batteries, attempts at aircraft electrification will lead to a considerable increase in aircraft operational empty weight; the larger the battery packs, the heavier the bare airframe.

5.1. Two-Engine Commercial Airliner Flown to and from a Long Runway

Consider the following approximation of a Boeing 737-MAX8: *Sref* = 1344 ft^2; *CD0* ~ 0.0250; *ARe* ~ 9.5; *VKTAS* = 460 knots (Mach 0.8 @ FL350), *TSFC* ~ 0.61 lbm/lbf-hr, *L/D* ~ 15.5. $CLmax_{T/O}$ ~ 1.95; $CLmax_{LD}$ ~ 2.7. *OEW* = 100,000 lbm; *MTOW* = 181,000 lbm; *MAXFUEL* = 46,500 lbm; *MAXPAYLOAD* = 45,400 lbm; *MLW* = 152,700 lbm. These parameters support a Breguet-equation-based payload–range chart, which roughly matches the advertised performance of a 2600 NM range capability with a 45,000 lbm payload; see Figure 5.

For a North American regional flight of 1500 NM to and from long, 10,000 ft runways with no obstacles, the 737-MAX8 can dispatch at ~165,000 lbm with its maximum 45,000 lbm payload; see the red circle in Figure 5. Under these circumstances, its field performance is more than adequate for both take-off (*CFL* = ~7200 ft) and landing (*LDR* = ~5000 ft after burning its mission fuel); its weight is neither limited by the structural certification (i.e., *MTOW* or *MLW*) nor the field performance. Since the predicted dry weather take-off is not a function of *VMCA*, no penalty arises as a byproduct of a substantial increase in low-speed thrust.

A statistically relevant collection of performance predictions may be built from a comprehensive parametric sweep (full factorial + 2000 converged-point Latin hypercube). The study varies relevant *k-factors*: k_{OEW} increases from 0% *MTOW* to 40% *MTOW*, step 10%; k_{TSFC} ranges from a 0% to a 90% reduction in fuel burn, step 10%; and k_{THRUST} varies from a 20% loss in low-speed thrust through to a 60% increase in low-speed thrust, step 5%. Analysis of the resulting collection reveals

the following. First, Figure 6a documents how aircraft payload capability is overwhelmingly dictated by the maximum landing weight certification; since landings are planned with most of the fuel consumed, the aircraft was designed so that its maximum landing weight (*MLW*) is considerably lower than its maximum take-off weight (*MTOW*). Aircraft are typically designed so that the *MLW* is somewhat greater than the sum of the baseline *OEW*, the maximum payload and the minimal fuel reserves. For the B737, *MLW* = ~152,700 lbm. In the trade study, we see how small that margin was.

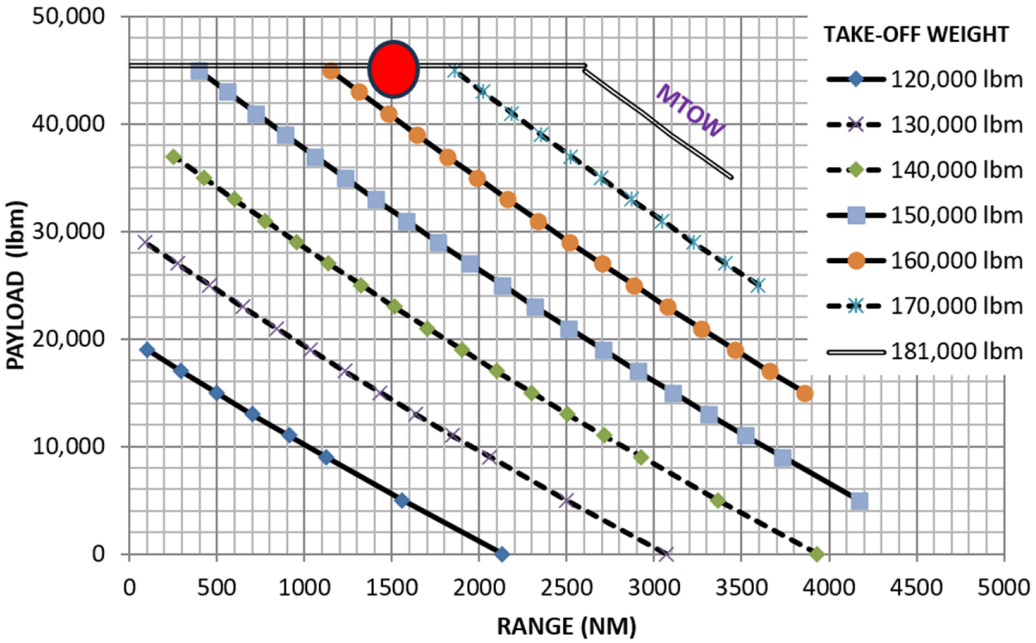


Figure 5. Breguet-equation-estimated performance of a B737-MAX8-inspired aircraft.

Figure 6a finds the trend where heavier *OEW* leads to smaller usable payloads. If *OEW* grows more than 25% of *MTOW*, safe dispatch with even zero payload becomes impossible. Common, repeated payload solutions obscure the grid-like nature of the full-factorial independent parameter variation (compare the blue dots for the full-factorial with the orange open-circles for the LHC); absent an *OEW* increase, the mission is not challenging enough to render changes in *T/W* or *TSFC* sufficient to preclude success when loaded to *MZFW* limits.

Figure 6b proves the correlation between mission specific range and effective propulsion system *TSFC*. At nominal engine efficiency, where k_{TSFC} = 0, the 737 has a mission specific range of 0.082 NM/lbm; the aircraft consumes ~18,300 lbm of fuel to perform its mission.

Figure 6c,d expose a lack of correlation between independent variations in take-off thrust (k_{THRUST} +/− 20%) or cruise TSFC (k_{TSFC} + 0/− 90%) and mission payload capability. This is made evident by the "random scatter" nature of the presented data: some combinations of parameters enable safe dispatch at maximum payload; other combinations cannot do so. Over the range of the *k-factors* studied, we see how a combination of factors (rather than fuel consumption savings alone) impacts usable payload. The "secondary effects" captured in this study are the independent variables not captured in a particular scatter plot. In the case of Figure 6c, the secondary effects are the impacts of *OEW* and *TSFC*. For Figure 6d, the secondary effects are the impacts of *OEW* and *Thrust*. Secondary effects above and beyond the independent variables used in this study are also expected to impact the results.

Taken together, we see that the *OEW* impact of a given technology is the critical parameter. Because an all-seats-occupied B737-8MAX economic mission (189 pax at 200 lbm/pax) implies a ~38,000 lbm payload, we see that this aircraft can tolerate no more than 5% *MTOW* growth in *OEW* (~9000 lbm) before it must offset payload to keep within the maximum landing weight limits.

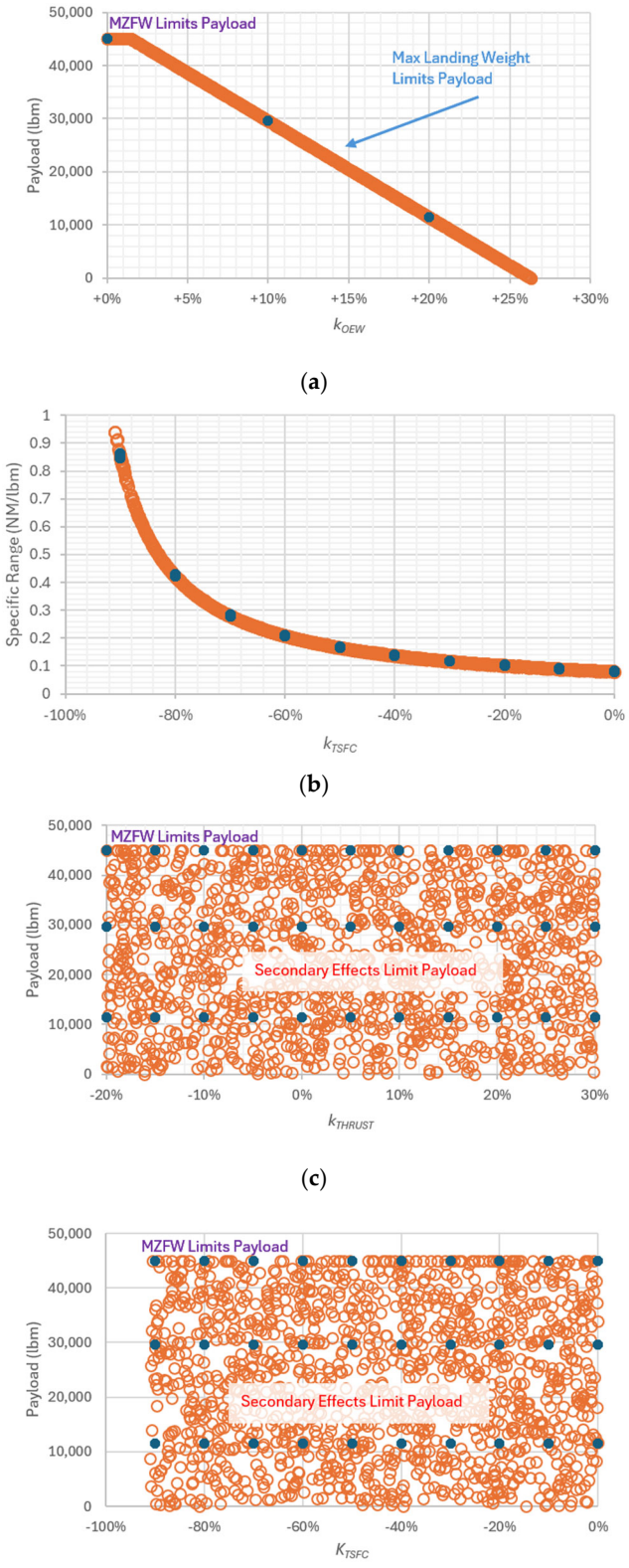


Figure 6. Two-engine airliner—long runway. Scatter plots are based on simultaneous *k-factor* variation representing %*OEW* increase, %change in cruise *TSFC* and %change in reference take-off thrust. Solid dots represent full-factorial candidate designs; open circles represent LHC sampled candidate designs. (**a**) Payload as a function of *OEW* gain expressed in terms of %*MTOW*, (**b**) specific range as a function of *TSFC*, (**c**) payload as a function of take-off thrust, and (**d**) payload as a function of cruise *TSFC*.

https://doi.org/10.3390/aerospace13050480

5.2. Two-Engine Commercial Airliner Flown from a Short Runway with a OEI Climb Gradient Constraint

Let us next consider the 737 operated under a weight-restricted dispatch scenario. If we refer back to the payload–range chart (Figure 5), we see that, absent any field performance constraints (take-off and arrival runway lengths and obstacle clearance restrictions), the baseline 737-MAX8 could fly a 500 NM mission with full payload with a planned take-off at ~152,000 lbm.

We next repeat the parameter sweep (full factorial + 2000 converged-point Latin hypercube) of the relevant *k-factors* (k_{OEW} increase, k_{TSFC} improvement and k_{THRUST} increase) for 500 NM operations to and from a 6052 ft runway with a 4.2% *OEI* climb gradient; in other words, from Runway 7 at KSBA. If the aircraft cannot comply with the requirements, the modeling tool will set the usable payload to 0 lbm.

Here, we see a new trend developing among compliant dispatch cases. As before, repeated payload solutions obscure the grid-like nature of the full-factorial independent parameter variation; the random variations from the Latin hypercube sampling scheme predominate the graphs. We also see striations, arising from this sampling strategy, develop in the dependent vs. independent variable plots.

Figure 7a has more scatter than Figure 6a; this indicates that, while the maximum payload capability is limited by the maximum landing weight, on a more challenging runway, secondary factors can limit payload even in the absence of an *OEW* increase. The scatter is induced by situations where landing limitations (i.e., *MLW* = 152,700 lbm) interact with the increase in *OEW*. Figure 7b indicates that the mission specific-range continues to correlate directly with the effective propulsion system *TSFC*. Figure 7c reveals that, while secondary factors continue to dominate the take-off thrust trade, if take-off thrust is degraded by 20%, no combination of assessed technology can enable a 45,000 lbm payload dispatch (see the red circled region of the plot) from KSBA and maintain the necessary *OEI* gradient. Figure 7d exposes a continued lack of correlation between independent variations in cruise *TSFC* (k_{TSFC} + 0/− 90%) and mission payload capability. This is made evident by the "random scatter" nature of the presented data; secondary factors predominate.

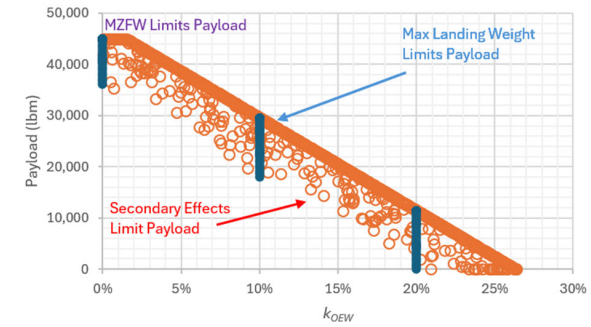
5.3. Four-Engine Transport Flown to and from a Long Runway

Next, we consider the following approximation of an older Lockheed L-100/C-130H aircraft: *Sref* = 1745 ft^2; *CD0* ~ 0.0300; *ARe* ~ 10; *VKTAS* = 250 knots, *TSFC* ~ 0.5 lbm/lbf-hr, *L/D* ~ 14.5. $CLmax_{T/O}$ ~ 2.15; $CLmax_{LD}$ ~ 2.45. *OEW* = 84,000 lbm; *MTOW* = 175,000 lbm; *MAXPAYLOAD* = 45,000 lbm; *MLW* = 155,000 lbm. Unlike many other transport category aircraft, which offer a multitude of high-lift options, the C-130 has only three flap settings: clean, take-off and landing. Functionally, it cannot make subtle trades of *CLmax* and drag to optimize field performance.

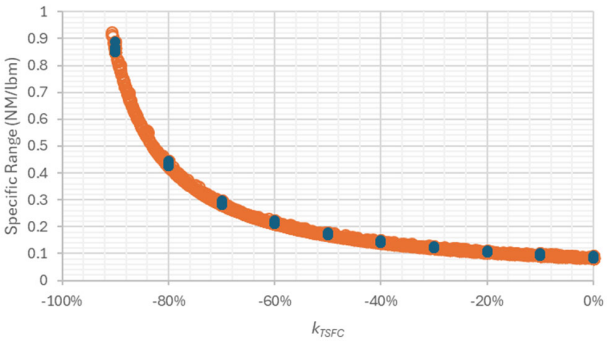
While the L-100/C-130 is a premier tactical transport, it is often flown to and from long runways. For this trade, we perform a parameter sweep (full factorial + 2000-point valid Latin hypercube) of the relevant *k-factors* (k_{OEW} increases from 0% *MTOW* to 40% *MTOW*, step 10%; k_{TSFC} ranges from a 0% to a 90% reduction in fuel burn, step 10%; and k_{THRUST} varies from a 20% loss in low-speed thrust through to a 60% increase in low-speed thrust, step 5%) for 1500 NM operations to and from a 10,000 ft runway, with only the basic MIL-3013B 2.5% *OEI* climb gradient constraint. Among compliant dispatch cases, we see the following trends.

As with the B737, repeated payload solutions obscure the grid-like nature of the full-factorial independent parameter variation; the random variations from the LHC sampling scheme predominate the graphs. We see that Figure 8a has a similar amount of scatter as the short-field B737 operations. Most of the evaluated designs cluster on a frontier where the maximum payload capability is fundamentally limited by both the maximum landing weight and the maximum zero-fuel weight: recall that the maximum payload arises from the difference between *MZFW* and *OEW*. We also see that secondary field-performance-related factors become increasingly important if a technology change increases *OEW* by more than 10% of *MTOW* (17,500 lbm). Figure 8b indicates that the mission specific range remains dominated by the effective propulsion system *TSFC;* the scatter evident in the correlation is a result of secondary factors (particularly weight growth), which can degrade fuel efficiency. Finally, the scatter revealed by Figure 8c indicates that moderate changes in take-off thrust need not degrade payload capability; some combinations of thrust, *OEW* and *TSFC* may even improve payload capability. Figure 8d exposes a continued lack of correlation between independent variations in cruise *TSFC* (k_{TSFC} + 0/− 90%) and mission payload capability. A large number of

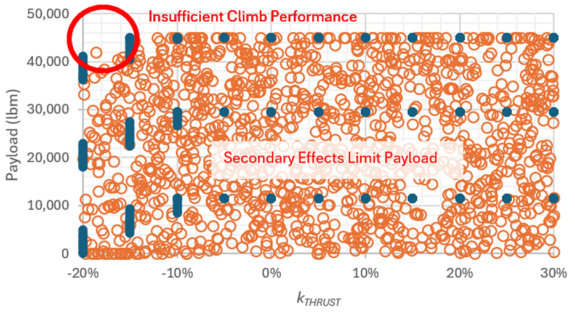
study conditions cluster at the 45,000 lbm *MZFW* limit; over the range of *k-factors* studied, a drastic reduction in fuel consumption may not be able to improve payload capability.



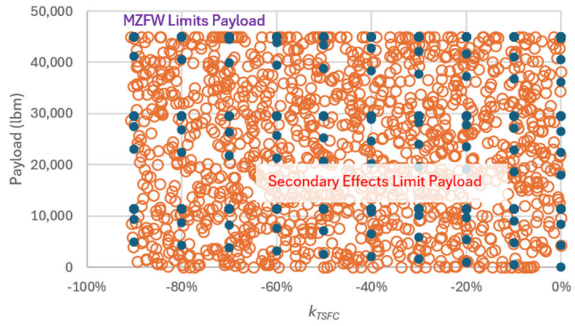
(**a**)



(**b**)

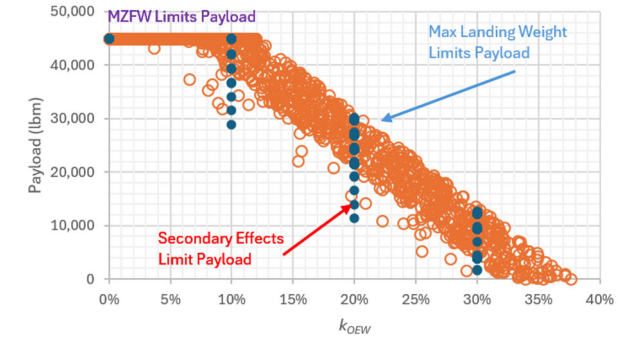


(**c**)

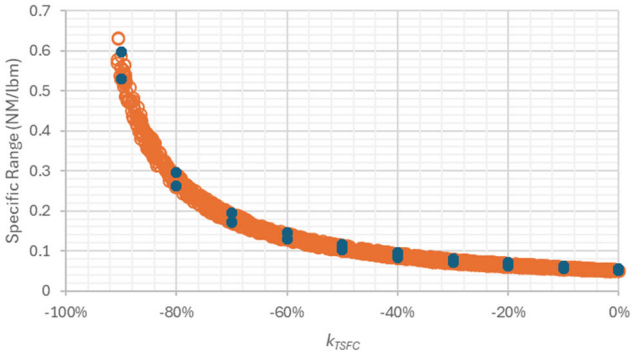


(**d**)

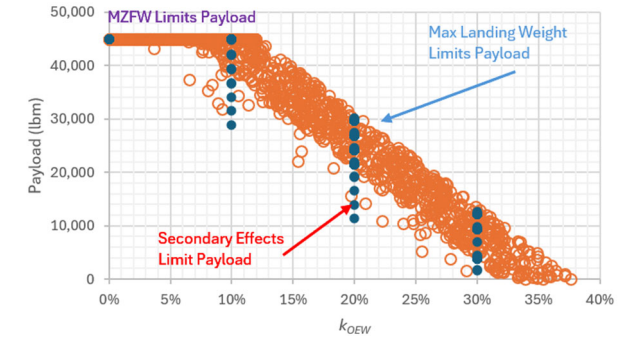
Figure 7. Two-engine airliner—short runway. Scatter plots are based on simultaneous *k-factor* variation representing %*OEW* increase, %change in cruise *TSFC* and %change in reference take-off thrust. Solid dots represent full-factorial candidate designs; open circles represent LHC sampled candidate designs. (**a**) Payload as a function of *OEW* gain expressed in terms of %*MTOW*, (**b**) specific range as a function of *TSFC*, (**c**) payload as a function of take-off thrust, and (**d**) payload as a function of cruise *TSFC*.



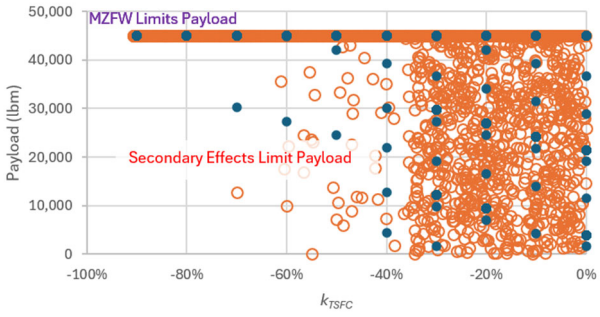
(**a**)



(**b**)



(**c**)



(**d**)

Figure 8. Four-engine transport—long runway. Scatter plots are based on simultaneous *k-factor* variation representing %*OEW* increase, %change in cruise *TSFC* and %change in reference take-off thrust. Solid dots represent full-factorial candidate designs; open circles represent LHC sampled candidate designs. (**a**) Payload as a function of *OEW* gain expressed in terms of %*MTOW*, (**b**) specific range as a function of *TSFC*, (**c**) payload as a function of take-off thrust, and (**d**) payload as a function of cruise *TSFC*.

5.4. Four-Engine Transport Flown to and from a Short Runway with an OEI Climb Gradient Constraint

Lastly, consider a L-100/C-130 transport, flown in its element—to and from a short runway surrounded by challenging obstacles. For this final trade, we perform a parameter sweep (full factorial + 2000 converged-point Latin hypercube) of the relevant *k-factors* (*OEW* increase, *TSFC* improvement and take-off thrust variation) for a 500 NM flight to and from a 4000 ft runway with a stringent 10% *OEI* climb gradient constraint. The baseline aircraft is weight-restricted to dispatch at ~116,000 lbm, limiting the payload to ~20,000 lbm.

Among compliant dispatch cases, we see newly emerging trends. First, Figure 9a develops additional scatter. If we contrast Figure 9a with Figure 8a, we can see a fundamentally different pattern emerge in the data—secondary technology factors no longer cluster near the frontier: *TSFC* benefits and take-off thrust now have a substantial impact on operational payload. The scatter in this plot arises where take-off field performance (i.e., the 4205 ft *TODA*), rather than *MLW*, controls the feasible solution and reduces the payload accordingly.

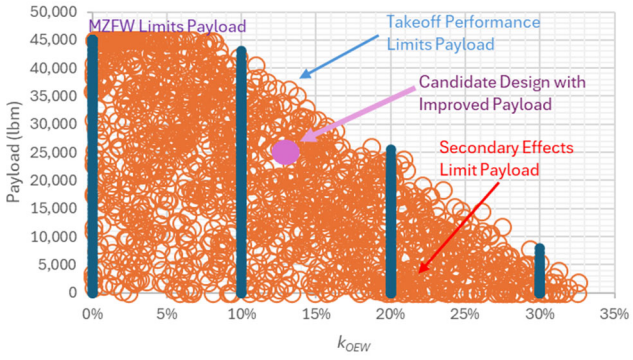
We can also see that a careful selection of technology can improve upon the reference ~20,000 lbm payload even if it comes with a severe *OEW* penalty. For example, the magenta circle found in Figure 9a represents a design which may safely dispatch a ~25,000 lbm payload (5000 lbm more than the baseline aircraft) at a 15% *MTOW* increase in *OEW* (a 26,250 lbm increase in *OEW*), provided that technology offers 30% mission fuel savings and a 60% increase in low-speed take-off thrust (reflected by the position of the magenta circle in Figure 9b–d).

Figure 9b indicates that the mission specific range remains dominated by the effective propulsion system *TSFC*, but the further increase in scatter (contrast Figure 9b with Figure 8b) is a byproduct of secondary factors (particularly weight growth) that degrade fuel efficiency. In particular, the increase in flight weight increases the dimensional magnitude of the induced drag, leading to a reduction in the specific range decorrelated from *TSFC*.

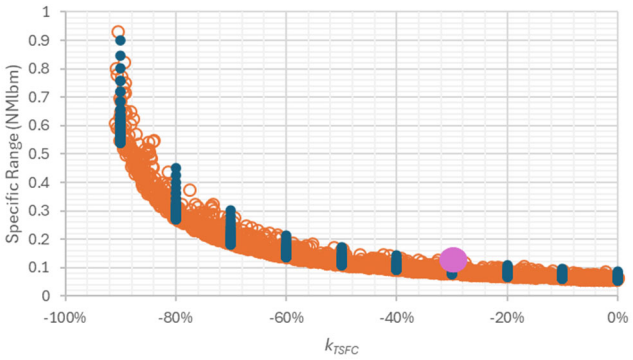
Figure 9c reveals a fundamentally different pattern than that seen above in Figure 8c. Note that the upper left quadrant of the chart has been depopulated of valid dispatch solutions; if take-off thrust degrades, no combination of foreseeable fuel consumption or *OEW* perturbations can safely depart with significant payload. The chart also reveals that a significant increase in available take-off thrust can improve the usable payload even in the presence of substantial gains in *OEW*.

Figure 9d demonstrates the pervasive lack of correlation between independent variations in cruise *TSFC* (k_{TSFC} + 0/− 90%) and mission payload capability. Note the increasing number of study conditions that cluster at 0 lbm payload; these are infeasible solutions to fly the required mission.

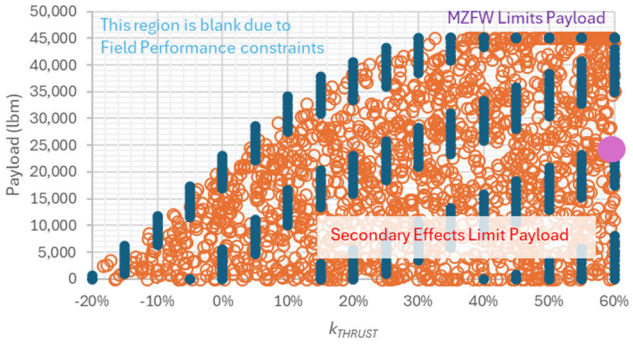
Figure 10 highlights further complexity relating to weight-limited dispatch. When holding baseline *TSFC* and *OEW* but varying take-off thrust, we see three distinct slopes present in the payload-vs-%increase in take-off thrust plot; Figure 10a. For this example, if take-off thrust degrades more than 10%, the aircraft becomes *OEI*-climb-gradient-limited. With a 20% reduction in take-off thrust, the usable payload drops to near-zero; any further reduction in thrust will ground the aircraft. Between −10% (degradation) and +50% (enhancement) take-off thrust increments, the aircraft is field-length-limited. When field length is limited, additional thrust enables safe dispatch at higher weights, thus increasing potential payload capability; the *OEI* climb gradient constraint is now inactive (see Figure 10b). Finally, above the +50% enhanced take-off thrust, the aircraft runs into its *MZFW*-imposed weight limit; both the take-off field length and *OEI* climb gradient constraints are inactive; see Figure 10b. Together, this figure demonstrates how the available payload response to thrust loading is not only non-linear, but has distinct piecewise breaks due to the engagement of changing constraints.



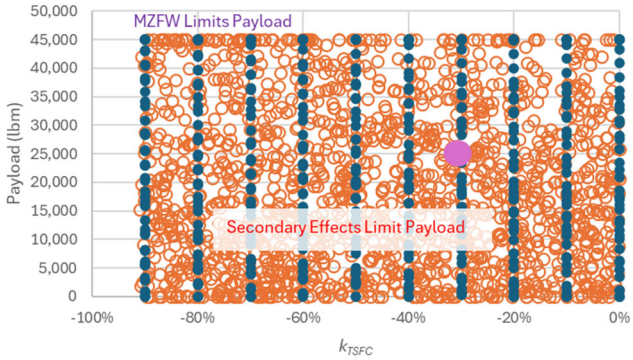
(**a**)



(**b**)

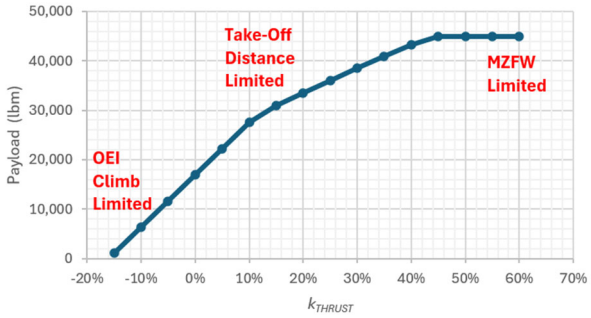


(**c**)

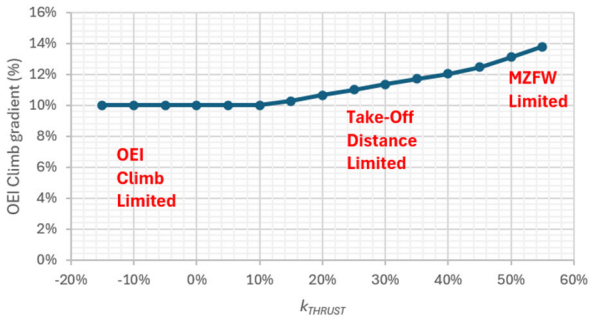


(**d**)

Figure 9. Four-engine transport—4000 ft runway with a 10% *OEI* gradient. Scatter plots are based on simultaneous *k-factor* variation representing %*OEW* increase, %change in cruise *TSFC* and %change in reference take-off thrust. Solid dots represent full-factorial candidate designs; open circles represent LHC sampled candidate designs. (**a**) Payload as a function of *OEW* gain expressed in terms of %*MTOW*, (**b**) specific range as a function of *TSFC*, (**c**) payload as a function of take-off thrust, and (**d**) payload as a function of cruise *TSFC*.



(**a**)



(**b**)

Figure 10. Four-engine transport—4000 ft runway with a 10% *OEI* gradient. (**a**) Sensitivity of payload capability to take-off thrust (baseline *OEW* and *TSFC*). (**b**) Sensitivity of the *OEI* climb gradient to take-off thrust (baseline *OEW* and *TSFC*).

6. Summary and Conclusions

Although it is essential to modern aircraft operations, the intentional dispatch of an aircraft where the end user trades the payload and/or range for field performance has not been prominently featured in classic design books. This paper provides the framework and foundation to apply this constraint at a conceptual design/technology portfolio screening level.

Weight-restricted operations occur whenever the planned payload and fuel load exceed the maximum allowable take-off weight for dispatch (runway and weather). The limitation on the payload ensures that the aircraft can safely perform its take-off and climb. On a commercial flight, a reduced payload means that passengers and/or baggage may be denied boarding. On a military flight, payload reductions will require a scale-back of operational objectives.

From our analysis of two parametrically varied derivative aircraft, operated under commercial or military rules, we see how stringent field performance constraints impact feasible dispatch. During weight-restricted operations, three parameters dominate trade studies: changes to low-speed thrust, changes to *OEW*, and changes in mission fuel burn. They control the basic success of the mission: if dispatch does not allow a flight to depart due to inadequate field performance, any theoretical changes of "technology" in economics, emissions, or noise become moot.

Our review of prior studies focusing on the application of retrofit hybrid electric propulsion systems to current production airframes notes a general lack of field performance constraints. Antcliff et al. is an exception that proves the rule: On the surface, it is a paper that considers a hybrid electric retrofit of an ATR-42-500. After the imposition of only modest field performance constraints, they necessitated a substantial increase in the wing area and an increase in *MTOW* to accompany the propulsion retrofit [39]. We suspect that the inclusion of field performance constraints following the dispatch weight-restriction approach found in this paper would lead other authors to fundamentally different conclusions.

In the four example cases we present, we show how changes in low-speed thrust, *OEW* and mission fuel consumption impact the usable payload of the aircraft. At present, we restrict ourselves to showing a series of individual independent/dependent variable scatter plots, as we have not discerned a format to visualize the design coupling in a single, more complex plot. In some

situations, a technology change that increases take-off thrust may allow the derivative aircraft to retain or even improve its usable payload over a defined mission, even if the technology imposes a substantial *OEW* increase. In other situations, we find that aircraft become extremely sensitive to *OEW*; technologies that do not directly result in weight savings will reduce usable payload. We also see that field-performance-imposed weight restrictions may arise from either take-off, climb-out or landing constraints; the activity of a constraint is extremely context-dependent on both the aircraft configuration and the reference mission used for the study.

In the future, the AFIT team plans to identify combinations of *k-factors*, using the dispatch weight limitation method shown here, that reflect specific tangible hybridization technology options. When we view the utility of candidate technologies through the prism of challenging commercial or military field performance constraints, we will develop new insights. As shown in the exemplary studies, it is important to carefully scale candidate propulsion technologies. If a system increases the low-speed thrust above the baseline value, it may provide a substantial improvement in payload capability (along with other side benefits), even if that technology is quite heavy. Yet, a substantial increase in *T/W* to compensate for *OEW* growth must not impact the minimum control airspeed (*VMCA*). If *VMCA* is too fast, an aircraft cannot dispatch to or from a runway no matter what its thrust or stall speed are. The studies shown here presume that engineers can implement a take-off thrust compensation system to mitigate *VMCA* issues without degrading usable thrust at typical take-off climb speeds. Conversely, a proposed system that decreases low-speed thrust may preclude permissible dispatch—an aircraft may be unsuitable for a mission no matter how impressive a technology appears when operated to and from long runways.

Funding: This work was funded by ARPA-E, part of the United States Department of Energy on an intergovernmental grant to the United States Air Force Institute of Technology, Prof. David Jacques, Principal Investigator.

Data Availability Statement: Numerical simulation data is self-contained within this article.

Conflicts of Interest: The author declares no conflicts of interest.

Approved for Public Release: Distribution Statement A. Approved for public release: distribution is unlimited. Docket Number: 88ABW-2025-0871. This material is declared a work of the U.S. Government and is not subject to copyright protection in the United States. The views expressed are those of the author and do not reflect the official guidance or position of the United States Government, the Department of Defense, the United States Air Force, or the United States Space Force.

Abbreviations

The following abbreviations are used in this manuscript:

Nomenclature

AEO	All-Engines-Operating
AGL	Height Above Ground Level (ft)
CFR	Code of Federal Regulations (the U.S. Government regulatory library)
FAA	Federal Aviation Administration (a U.S. Government agency)
GRAD	Climb Gradient (%)
MLW	Maximum Landing Weight (lbm)
MTOW	Maximum Take-Off Weight (lbm)
MZFW	Maximum Zero-Fuel Weight (lbm)
OEI	One-Engine-Inoperative (the most critical engine for controllability) and performance
OEW	Operational Empty Weight (lbm)
SPECIFICRANGE	Distance Traveled per Pound Fuel Consumed (NM/lbm)
k_{OEW}	k-factor scaling Operational Empty Weight
k_{TSFC}	k-factor scaling Mission Fuel Consumption
k_{THRUST}	k-factor scaling Low-Speed Take-Off Thrust

Distances

CFL	Critical Field Length (ft)
LDA	Landing Distance Available (ft)
TODA	Take-Off Distance Available (ft)
Speeds	
*V*2, *Vobs*	Obstacle Clearance Speed—the target airspeed during an *OEI* continued take-off (knots)
VMCA	Minimum-control speed in the Air—T/O Configuration (knots)
VMCL	Minimum-control speed in the Air—Landing Configuration (knots)
Vs	Stall Airspeed—where *CL* = *CLmax* (knots)

References

1. Kirby, M.L.; Mavris, D.N. An Approach for the Intelligent Assessment of Future Technology Portfolios. In Proceedings of the 40th AIAA Aerospace Sciences Meeting & Exhibit, Reno, NV, USA, 14–17 January 2002; AIAA 2002-0515. [CrossRef]
2. Mavris, D.N.; Phan, L.L.; Garcia, E. Formulation and Implementation of an Aircraft-System-Subsystem Interrelationship Model for Technology Evaluation. *Environment* **2006**, *21*, 35–36.
3. Cleveland, F.A. Size effects in conventional aircraft design. *J. Aircr.* **1970**, *7*, 483–512. [CrossRef] [PubMed]
4. Raymer, D.P. *Aircraft Design: A Conceptual Approach*, 6th ed.; AIAA: Reston, VA, USA, 2018.
5. Takahashi, T.T. *Aircraft Performance and Sizing, Vol. II: Applied Aerodynamic Design*; Momentum Press: New York, NY, USA, 2016.
6. Lan, C.T.E.; Roskam, J. *Airplane Aerodynamics & Performance*; DAR Corporation: Lawrence, KS, USA, 2003.
7. Roskam, J. *Airplane Design Part 1: Preliminary Sizing of Airplanes*; DAR Corporation: Lawrence, KS, USA, 2015.
8. Nicolai, L.M. *Fundamentals of Aircraft Design*; METS Inc.: San Jose, CA, USA, 1975.
9. Torenbeek, E. *Synthesis of Subsonic Aircraft Design*; Springer: Dordrecht, The Netherlands, 1982.
10. Brandt, S.A. *Introduction to Aeronautics: A Design Perspective*, 3rd ed.; AIAA: Reston, VA, USA, 2015.
11. Available online: https://arpa-e.energy.gov/programs-and-initiatives/view-all-programs/ascend (accessed on 2 March 2026).
12. McVey, P. Feasibility Study of a Hybrid-Electric Propulsion System for the C-130 Hercules. Master's Thesis, Air Force Institute of Technology, Wright-Patterson AFB, OH, USA, 2026; AFIT-ENV-MS-26-M-146.
13. Pham, D.D.V.; Listgarten, N.S.; Zilliac, G.G.; Go, S.; Bowles, J.V.; Jansen, R.H. Parametric Modeling and Mission Performance of a True Parallel Hybrid Turboprop Aircraft for Freighter Operations. In Proceedings of the AIAA Aviation Forum and Ascend, Las Vegas, NV, USA, 29 July–2 August 2024; AIAA 2024-3581. [CrossRef]
14. Listgarten, N.S.; Pham, D.D.V.; Natividad, C.A.D.; Margolis, B.W.; Lyons, K.R.; Garcia, J.A.; Bowles, J.V.; Russell, C.E. Parallel Hybrid Turboprop Performance Modeling and Optimization. In Proceedings of the AIAA SCITECH 2025 Forum, Orlando, FL, USA, 6–10 January 2025; AIAA 2025-1435. [CrossRef]
15. Jansen, R.H.; DeBock, P.; Stalcup, E.; Dever, T.; Wilhite, J.M.; Pham, D.D.V.; Wishart, J.M. Hybrid Electric Turboprop Commercial Freighter Opportunity. In Proceedings of the AIAA SCITECH 2025 Forum, Orlando, FL, USA, 6–10 January 2025; AIAA 2025-1642. [CrossRef]
16. Takahashi, T.T. Development of Improved Empirical Take-Off Equations. *Aerospace* **2025**, *12*, 695. [CrossRef]
17. Peak, R.; Bodner, D.; Bishop, C.; Ender, T.; McDermott, T.; McGinnis, L.; Paredis, C.; Rouse, W. Overview of Systems Engineering Research at Georgia Tech. In Proceedings of the 2nd Annual SERC Research Review Conference, College Park, MD, USA, 9–10 November 2010. Available online: https://apps.dtic.mil/sti/html/tr/ADA545262/ (accessed on 15 May 2026).
18. Morris, E.; Williams, M.; Ahlberg, J.B.; Chappell, R.; McNamara, R.S.; Glass, P. *The Fog of War: Eleven Lessons from the Life of Robert S. McNamara*; Sony Pictures Classics (Film): New York, NY, USA, 2004.
19. Anonymous. *Operational Research in the British Army 1939–1945; Report C67/3/4/48; UK National Archives File WO291/1301*; UK National Archives: Richmond, UK, 1947.
20. Gannon, M. *Black May: The Epic Story of the Allies' Defeat of the German U-Boats in May 1943*; Naval Institute Press: Annapolis, MD, USA, 2010.
21. Schmit, L.A. Structural Design by Systematic Synthesis. In Proceedings of the 2nd Conference on Electronic Computation, ASCE, Pittsburgh, PA, USA, 8–9 September 1960; pp. 105–132.
22. Kirby, M.R.; Mavris, D.N. Forecasting the Impact of Technology Infusion on Subsonic Transport Affordability. In Proceedings of the World Aviation Congress & Exposition, Anaheim, CA, USA, 28 September 1998; SAE Paper No. 985576. [CrossRef]
23. Kirby, M.R.; Mavris, D.N. A Technique for Selecting Emerging Technologies for a Fleet of Commercial Aircraft to Maximize R&D Investment. In Proceedings of the World Aviation Congress & Exposition, Seattle, WA, USA, 11 September 2001; SAE Paper No 2001-01-3018. [CrossRef]
24. Mavris, D.N.; Bandte, O.; DeLaurentis, D.A. Robust Design Simulation: A Probabilistic Approach to Multidisciplinary Design. *J. Aircr.* **1999**, *36*, 298–307. [CrossRef] [PubMed]

25. Cavanaugh, S.; Chytka, T.; Arcara, P.; Jones, S.; Stanley, D.; Wilhite, A. NASA Langley Systems Analysis & Concepts Directorate Technology Assessment/Portfolio Analysis. In Proceedings of the 11th AIAA/ISSMO Multidisciplinary Analysis and Optimization Conference, Portsmouth, VA, USA, 6–8 September 2006; AIAA 2006-7029. [CrossRef]
26. Burgaud, F.; Frank, C.P.; Mavris, D.N. An Aircraft Development Methodology Aligning Design Strategy to Support Key Decision Making. In Proceedings of the 57th AIAA/ASCE/AHS/ASC Structures, Structural Dynamics, and Materials Conference, San Diego, CA, USA, 4–8 January 2016; AIAA 2016-1661. [CrossRef]
27. Jimenez, H.; Mavris, D. Pareto-Optimal Aircraft Technology Study for Environmental Benefits with Multi-Objective Optimization. *J. Aircr.* **2017**, *54*, 5. [CrossRef]
28. Cinar, G.; Cai, Y.; Chakraborty, I.; Mavris, D.N. Sizing and Optimization of Novel General Aviation Vehicles and Propulsion Systems Architectures. In Proceedings of the 2018 Aviation Technology, Integration, and Operations Conference, Atlanta, Georgia, 25–29 June 2018; AIAA 2018-3974. [CrossRef]
29. Liu, Y.; Elham, A.; Horst, P.; Hepperly, M. Exploring Vehicle Level Benefits of Revolutionary Technology Progress via Aircraft Design and Optimization. *Energies* **2018**, *11*, 166. [CrossRef]
30. Lim, D.; Lee, D.; Yee, K. Technology Portfolio Assessment with Uncertainty Consideration for Advanced Air Mobility. In Proceedings of the AIAA AVIATION 2022 Forum, Chicago, IL, USA, 27 June–1 July 2022; AIAA 2022-3660. [CrossRef]
31. Jouannet, C.; Amadori, K.; Bäckström, E. Selection of Future Technologies During Aircraft Conceptual Design. In Proceedings of the 55th AIAA Aerospace Sciences Meeting, Grapevine, TX, USA, 9–13 January 2017; AIAA 2017-0233. [CrossRef]
32. Amadori, K.; Bäckström, E.; Jouannet, C. Future Technologies Prioritization for Aircraft Conceptual Design. In Proceedings of the 2018 AIAA Aerospace Sciences Meeting, Kissimmee, FL, USA, 8–12 January 2018; AIAA 2018-1746. [CrossRef]
33. Amadori, K.; Bäckström, E.; Jouannet, C.; Bianchi, D. Uncertainty Management in Technologies Prioritization for Future Aircraft Program. In Proceedings of the AIAA Scitech 2020 Forum, Orlando, FL, USA, 6–10 January 2020; AIAA 2020-0019. [CrossRef]
34. Bianchi, D.H.B.; Amadori, K.; Backstrom, E.; Jouannet, C.; Secco, N.R. An Uncertainty-Based Framework for Technology Portfolio Selection for Future Aircraft Program. In Proceedings of the AIAA Scitech 2021 Forum, Virtual, 19–21 January 2021; AIAA 2021-1479. [CrossRef]
35. Abu Salem, K.; Palaia, G.; Quarta, A.A. Review of Hybrid-Electric Aircraft Technologies and Designs: Critical Analysis and Novel Solutions. *Prog. Aeronaut. Sci.* **2023**, *141*, 100924. [CrossRef]
36. Friedrich, C.; Robertson, P.A. Hybrid-Electric Propulsion for Aircraft. *J. Aircr.* **2015**, *52*, 176–189. [CrossRef]
37. Wroblewski, G.E.; Ansell, P.J. Mission analysis and emissions for conventional and hybrid-electric commercial transport aircraft. *J. Aircr.* **2019**, *56*, 1200–1213. [CrossRef]
38. Voskujl, M.; van Bogaert, J.; Rao, A.G. Analysis and design of hybrid electric regional turboprop aircraft. *CEAS Aeronaut. J.* **2018**, *9*, 15–25. [CrossRef]
39. Antcliff, K.R.; Guynn, M.D.; Marien, T.; Wells, D.P.; Schneider, S.J.; Tong, M.J. Mission Analysis, and Aircraft Sizing of a Hybrid-Electric Regional Aircraft. In Proceedings of the 54th AIAA Aerospace Sciences Meeting, San Diego, CA, USA, 4–8 January 2016; AIAA 2016-1028. [CrossRef]
40. Recine, C.J.; Pham, D.D.V.; Bowles, J.V.; Lyons, K.R.; Margolis, B.W.L.; Garcia, J.A. Analysis and Optimization of Baseline Single Aisle Aircraft for Future Electrified Powertrain Flight Demonstration Comparisons. In Proceedings of the AIAA AVIATION 2023 Forum, San Diego, CA, USA, 12–16 June 2023; AIAA 2023-3367. [CrossRef]
41. *14 CFR § 25*; Airworthiness Standards: Transport Category Airplanes. United States Government Printing Office: Washington, DC, USA, 2025.
42. *MIL STD-3013B*; Department of Defense Standard Practice: Glossary of Definitions, Ground Rules, and Mission Profiles to Define Air Vehicle Performance Capability. Department of Defense: Washington, DC, USA, 2008.
43. Available online: https://skyvector.com/airport/EGLC/London-City-Airport (accessed on 2 March 2026).
44. Anonymous. *Embraer 190 Airport Planning Manual; APM-1901, Rev. 24*; Embraer S.A.: Sao Jose dos Campos, Brazil, 2024.
45. Available online: https://www.airnav.com/airport/CYTZ (accessed on 2 March 2026).
46. Anonymous. *DASH-8 Series 400 Airport Planning Manual; PSM 1-84-13, Rev. 4*; Bombardier: Downsview, ON, Canada, 2014.
47. Anonymous. Southwest Airlines Corporate Facts. *Southwest Airlines*; Dallas, TX, USA, 30 June 2025. Available online: https://www.swamedia.com/vforcesite/cms/delivery/media/MC5SHG3HNX2FFRVLRCQTZRDPWU7E?version=9.1&channelId=0apHu000000IWrs (accessed on 2 March 2026).
48. Anonymous. *737 MAX Airplane Characteristics for Airport Planning; D6-38A004, Rev D*; Boeing Commercial Airplanes: Seattle, WA, USA, 2019.
49. Available online: https://www.airnav.com/airport/KSBA (accessed on 2 March 2026).
50. Available online: https://www.airnav.com/airport/KMDW (accessed on 2 March 2026).
51. Available online: https://www.airnav.com/airport/l70 (accessed on 2 March 2026).
52. Image Adapted from Source Document Generated. Available online: https://nationalmap.gov (accessed on 15 May 2026).

53. Anonymous. Lockheed Martin Completes Final Tests on C-130J Stick-Pusher. *Flight Global*. 7 October 1997. Available online: https://www.flightglobal.com/lockheed-martin-completes-final-tests-on-c-130j-stick-pusher/15022.article (accessed on 2 March 2026).
54. Anonymous. 737 MAX Software Update. Boeing, Undated. Available online: https://www.boeing.com/commercial/737max/737-max-update/737-max-software-updates (accessed on 2 March 2026).
55. Anonymous. *Flight Manual USAF Series C-130J (Long) Aircraft; TO 1C-130(C)J-1-1, Rev. 1*; Lockheed-Martin: Marietta, GA, USA, 2012.
56. Takahashi, T.T. Development of Improved Empirical Landing Equations for Conceptual Design. *Aerospace* **2026**, *13*, 390. [CrossRef]
57. Takahashi, T.T. Revisiting Roskam's Empirical Predictions for Landing Distance. In Proceedings of the AIAA Aviation 2021 Forum, Virtual, 2–6 August 2021; AIAA 2021-2447. [CrossRef]

Disclaimer/Publisher's Note: The statements, opinions and data contained in all publications are solely those of the individual author(s) and contributor(s) and not of MDPI and/or the editor(s). MDPI and/or the editor(s) disclaim responsibility for any injury to people or property resulting from any ideas, methods, instructions or products referred to in the content.